

# Dynamics in a low-temperature glass: Fast generation and detection of optical holes

K. A. Littau,<sup>a)</sup> M. A. Dugan, S. Chen, and M. D. Fayer  
*Department of Chemistry, Stanford University, Stanford, California 94305*

(Received 26 July 1991; accepted 27 November 1991)

High-resolution, fast optical hole-burning results are reported for the amorphous system cresyl violet in ethanol glass at 1.3 K. Holes are burned and detected using a novel technique which allows precise detection of narrow ( $\sim 0.03 \text{ cm}^{-1}$ ), shallow ( $\sim 1\%$ ) holes  $10 \mu\text{s}$  to  $50 \text{ ms}$  after their generation. The technique is described in detail along with careful tests demonstrating the validity of its results. The hole width is observed to increase linearly with time when plotted against log time. Using the four time correlation function description of optical hole burning, the time-dependent increase in hole width (spectral diffusion) is shown to arise from a broad distribution of fluctuation rates in the glass with the probability of having a fluctuation at rate  $R$  proportional to  $1/R$ . The  $10 \mu\text{s}$  to  $50 \text{ ms}$  data is combined with hole-width data spanning the range  $100 \text{ ms}$  to  $10\,000 \text{ s}$  and with two-pulse picosecond photon echo data. The two-pulse photon echo linewidth is calculated by extrapolating the fluctuation rate distribution obtained from the hole-width data to short times. The results are in excellent agreement with experimental echo results. The combined data from the two sets of hole-burning experiments provides a detailed description of the glass dynamics over nine decades of time,  $10\,000 \text{ s}$  to  $10 \mu\text{s}$ . Together with the two-pulse photon echo results, the data provide information on the glass dynamical behavior over seven decades faster in time as well. The net result is a description of the dynamics in low-temperature ethanol glass on time scales spanning 16 decades.

## I. INTRODUCTION

This paper presents the results of waiting-time- ( $T_w$ ) dependent hole-burning experiments on the system cresyl violet in glassy ethanol- $d$  (ethanol with the hydroxy hydrogen replaced by deuterium). The  $T_w$  dependence, that is, the dependence of the hole linewidth on the waiting time between burning and detecting the hole, of cresyl violet in ethanol- $d$  has been reported in detail earlier in the range  $0.1 \text{ s} < T_w < 10\,000 \text{ s}$ , and a preliminary report has been given for the range  $10 \mu\text{s} < T_w < 0.1 \text{ s}$ .<sup>1</sup> By varying the waiting time in hole-burning experiments between  $0.1$  and  $10\,000 \text{ s}$ , the glass fluctuation rate distribution,  $P(R)$  (the probability of having a fluctuation with rate  $R$ ) between  $10^{-4}$  and  $10 \text{ Hz}$  was determined. The rate distribution in this region was revealed to be log normal. In this paper high-resolution hole-burning experiments and associated theoretical considerations are presented for the range  $10 \mu\text{s} < T_w < 0.1 \text{ s}$ . A novel technique for quickly burning and detecting optical holes will be described in detail along with thorough tests of the validity of the results.

The dynamics of glasses and supercooled liquids, as well as other complex systems such as liquids and proteins, are generally characterized by a very broad distribution of relaxation times.<sup>2-14</sup> The results of stress-relaxation experiments provide good examples of this.<sup>4</sup> These kinds of mechanical experiments are quite useful in examining the dynamic spectrum of glasses at relatively high temperatures. Other experiments such as the response of ionic glasses to an applied

current or dielectric relaxation of glasses also prove useful.<sup>4-7</sup> With few exceptions,<sup>6,7</sup> however, these techniques are not suited to studying the dynamic properties of glasses at low temperature. Furthermore, these methods cannot cover a very broad range of time scales, and therefore they cannot examine the very broad range of relaxation rates that can occur in glasses and other complex systems.

Low-temperature studies of time-dependent properties have consisted mostly of time-independent thermodynamic measurements, the results of which are interpreted in terms of low-frequency glassy modes with a broad distribution of fluctuation rates. Temperature-dependent specific-heat measurements of glasses are classic examples of this.<sup>8-11</sup> While these experiments are sensitive to the dynamics of glasses, they effectively integrate the time response of the system across several decades. Thus, any time-dependent information is lost. Nevertheless, in order to explain the results of the thermodynamic measurements, specifically the non-Debye heat capacities of inorganic glasses, Anderson, Halperin, and Varma<sup>15</sup> and Phillips<sup>16</sup> used the concept of a broad distribution of dynamic rates in the two-level system (TLS) model of glass dynamics. The supposition is that a glass contains many TLS's; the ensemble of TLS's exhibits broad distributions of energies and relaxation rates (tunneling parameters). A TLS is described by an asymmetric double-well potential with an energy asymmetry  $E$  and a tunneling parameter between the wells,  $\lambda$ . Thus, each TLS will have a different activation energy and fluctuation rate. In the original TLS model the distributions of energies and tunneling parameters were assumed to be constant. This was sufficient to model the limited thermodynamic data available at

<sup>a)</sup> Present address: AT&T Bell Laboratories, Murray Hill, NJ 07974.

that time. However, more realistic, system-dependent distribution functions are required to successfully model the vast amount of data now available. Nevertheless, this model explained the low-temperature glass thermodynamic data quite well, but provided only indirect evidence for a broad distribution of fluctuation rates.

Subsequently, low-temperature dielectric relaxation<sup>6,7</sup> and time-dependent heat-capacity measurements<sup>17-20</sup> gave the first direct evidence of broad fluctuation rate distributions. It should be noted that the validity of the heat-capacity measurements have been called into question.<sup>21</sup> Nevertheless, the time dependence of low-temperature glass physical properties was conclusively demonstrated. Spectroscopic techniques were also employed and proved useful. Acoustic experiments such as phonon echoes<sup>22</sup> and ultrasonic attenuation<sup>23-25</sup> in addition to optical techniques such as hole burning<sup>26-28</sup> and fluorescence line narrowing<sup>29</sup> are good examples of this. However, these techniques again did not directly probe the distribution of rates since they either integrated the response of the system over a wide range of times or probed only a narrow band of rates (a single time or narrow range of times).

These limitations were sometimes inherent properties of the experiments. Fluorescence line narrowing, for example, is limited to probing rates on the order of the inverse of the fluorescence lifetime. In principle, hole-burning spectroscopy can investigate an extremely broad range of solvent fluctuation rates. Hole burning has been shown theoretically to be the frequency domain equivalent to the time-domain stimulated photon echo (three-pulse echo) experiment. The four-time correlation function that describes the hole-burning experiment is the Fourier transform of the correlation function that describes the stimulated echo third-order polarization. Hole burning is sensitive to all fluctuations faster than the waiting time ( $T_w$ ) between burning and reading the hole and slower than the two-pulse echo dephasing time.<sup>30</sup> This was not recognized until relatively recently. Thus, waiting times were usually longer than 100 s and were never varied. Breinl, Friedrich, and Haarer performed the first  $T_w$ -dependent hole-burning experiment and noted that the hole broadens logarithmically in the range of a few minutes to several days.<sup>14</sup> Still, the true utility of this technique had not been exploited.

Soon after the work of Breinl, Friedrich, and Haarer, time-resolved coherence experiments began to be used to study low-temperature glass dynamics. Accumulated grating echoes,<sup>31,32</sup> two-pulse photon echoes,<sup>33</sup> and stimulated photon echoes<sup>34-36</sup> were the first to be reported. These techniques were also limited in the range of relaxation rates they could study. For example, the decay measured in a photon echo experiment is sensitive to rates on the order of the reciprocal of the delay time between the pulses in the sequence.<sup>30,37,38</sup> However, two-pulse echo results were compared to hole-burning data with some success in determining the fluctuation rate distribution.<sup>30</sup> The experiments described here and previously<sup>1,39</sup> are the first detailed uses of spectroscopic results in mapping the fluctuation rate distribution of a low-temperature glass. Unlike in Ref. 39, where the recovery of a transient hole was measured at a single

frequency, the experiments detailed here record hole widths as a function of time. The ability to measure dynamical events over several decades of time is central to the theme of this paper. To this end, reference is made to the work of Scher, Shlesinger, and Bendler,<sup>40</sup> where transient photocurrent experiments on amorphous semiconductors have yielded dispersive transport and relaxation dynamics over 6-10 decades.

Understanding dynamics in glasses and other complex systems, that have very broad and unknown fluctuation rate distributions, is fundamentally different from the more conventional problem of dynamics in crystalline solids. In a crystal the fluctuations arise from the phonon modes that collectively act as a heat bath. At low temperatures the phonon modes are well characterized by a Debye density of states. The full phonon spectrum of a crystal can be measured with neutron scattering. Therefore the fluctuation rate distribution is known. At low temperature it is proportional to  $\omega^2 d\omega$ . Understanding optical linewidths (dephasing) or other dynamical phenomena involves determining the mechanism and strength of coupling of the subsystem of interest to the phonon heat bath. In a glass both the fluctuation rate distribution and the coupling of the optical center to the environment are unknowns.

Elucidating the fluctuation rate distribution is of fundamental importance in understanding glasses. When the TLS model was first introduced, it was noted that a flat distribution of TLS energies and fluctuation rates would account for the observed properties of glasses at low temperature known at that time. The temperature dependence of thermodynamic, acoustic, and spectroscopic properties of glasses have since been studied much more extensively.<sup>9-13,22-36,41-43</sup> Usually the temperature dependences of these results differ slightly from what the TLS theory coupled with these simple distribution functions predicts. For example, the constant distribution of TLS energy splittings (equal probability of any splitting) originally proposed predicts a linear temperature dependence for heat capacities<sup>15,16</sup> and for hole-burning linewidths.<sup>41</sup> The actual dependences of these quantities are usually somewhat superlinear.  $T^{1.3}$  is a common result.<sup>41-43</sup> In order to account for this, different distributions of TLS energies and fluctuation rates have been proposed.<sup>44-47</sup> These distributions have been successful in modeling the various experimental results. However, the validity of these theories could not be tested since no experiment existed to actually measure the distribution of fluctuation rates in these systems.

The  $T_w$ -dependent experiments introduced in this paper have that ability. Now theories of glass dynamics can be tested against the experimentally determined fluctuation rate distributions. The original TLS distribution functions predicted a  $1/R$  density of fluctuation rates. The results reported previously for very slow fluctuation rates in ethanol<sup>1</sup> yield a log normal distribution. The data reported in Sec. III extend the knowledge of the fluctuation rate distribution to substantially larger rates. The results indicate that the probability rate distribution follows a  $1/R$  behavior for rates between  $10^{12}$  and  $10^1$  Hz. The significance of this is also discussed in Sec. III.

## II. EXPERIMENTAL PROCEDURES

The sample studied was a  $1.2 \times 10^{-4} M$  solution of crexyl violet (Exciton) in ethanol-*d*. Previous work has found the hole width to be independent of concentration in this range.<sup>1</sup> It should be noted that previous experiments have determined that the low-temperature dynamics of ethanol-*d* are identical to those of ethanol.<sup>1,30,48</sup> Ethanol-*d* was chosen because it has factor of  $\sim 20$  lower *persistent* hole-burning efficiency.<sup>30,48</sup> This allowed transient holes to be recorded repeatedly on the sample without forming a substantial persistent hole. After being placed in a 1 mm spectroscopic cuvette, the sample was quickly cooled to liquid-helium temperatures in a <sup>4</sup>He bath cryostat. The cooling rate was rapid enough to avoid formation of the alternate glassy phase of ethanol that has been observed previously in thermodynamic and optical experiments.<sup>49,50</sup>

All spectra were recorded on the red side of the O–O absorption at 620 nm. This is well to the red of the absorption maximum at 610 nm.<sup>48</sup> The optical density of the sample at this wavelength was 0.6. The laser source for this experiment was a Coherent model 599-21 scanning single-mode dye laser pumped by an Innova 90-5 argon-ion laser run in all-lines mode. The Ar<sup>+</sup> laser was operated in this fashion so that some of the light could be split off without affecting the dye laser performance. This extra light was used to erase accumulated persistent holes as is described later.

The purpose of this experiment is to burn and detect narrow spectral holes with waiting times faster than 100 ms. Holes with waiting times between 100 ms and 10 000 s were detected previously.<sup>1</sup> The method used to record the results reported in Ref. 1 involved burning a hole with a short laser pulse (on the order of 10 ms) and scanning the laser frequency across the hole spectrum after a variable waiting time. Because the laser had to be scanned to record the holes (maximum scan rate  $\approx 100$  MHz/ms), spectra could not be recorded with waiting times faster than  $\sim 100$  ms.

In order to record holes with shorter waiting times, a new method was required. Previously, workers have recorded transient spectral holes quite simply. Using a short, relatively narrow-band pump pulse, a hole was burned and then was quickly detected with a broadband light source and a monochromator.<sup>51</sup> This was used primarily because the systems studied exhibited only transient hole burning (i.e., persistent spectral holes could not be burned), not because the researchers were interested in the time dependence of the hole linewidth.<sup>51</sup> This method (monochromator detection) would not be practical for detecting the narrow spectral holes studied here. Holes can be as narrow as 200 MHz in these glasses. This corresponds to  $0.007 \text{ cm}^{-1}$ . The ability to detect small changes in linewidth for these narrow holes is well beyond the resolution of monochromators.

To detect these narrow spectral holes without scanning the laser, the experiment was performed with two beams of different frequencies. One short intense beam burned the hole, and the second, a weak cw probe, read the hole. The reading beam was not scanned but measured the time response of the absorption *at a single frequency*. Thus, instead of measuring the entire spectrum of the hole at certain discrete times, the entire transient optical density is measured

at certain discrete frequencies. Important here is that the entire hole (assumed symmetric) is reconstructed at different weighting times. The absorption recovery at a given frequency can be influenced by such processes as spontaneous hole filling or persistent hole formation which may make the technique detailed in Ref. 39 less certain. The light from a single laser source was split into two beams and the frequency of one was shifted relative to the other with an acousto-optic modulator (AOM). The method is described in detail below.

The experimental apparatus is diagrammed in Fig. 1. The output of the CR599-21 was amplitude stabilized using an acousto-optic modulator controlled by a reference photodiode and feedback circuit. By this method, fast fluctuations and long-term drift were stabilized to better than  $\pm 2\%$ . The light was then split equally into two beams. The first, dubbed the burning beam, was amplitude modulated by two 40 MHz acousto-optic modulators (AOM's) and a mechanical shutter. The AOM's had a combined  $5 \times 10^5:1$  dynamic range of attenuation and a time response of better than  $1 \mu\text{s}$ . The mechanical shutter had a time response better than 1 ms. The AOM's were used to create the short burning pulses, and the shutter blocked the weak leakage light when the burning beam was not required. Since the laser output was amplitude stabilized, the burn pulse energy was kept constant to within a few percent.

The second beam, called the reading beam, passed through a variable attenuator, a frequency shifter, a mechanical shutter, and a spatial filter before reaching the sample. The variable attenuator was a polarizer, half-wave plate, polarizer combination which had a dynamic range of  $\sim 10^5:1$ . The frequency shifter was an AOM driven at 300 MHz. The frequency of the reading beam could be shifted in increments of 300 MHz by successively passing the diffracted beam back through the modulator. The crystal's dimensions were large

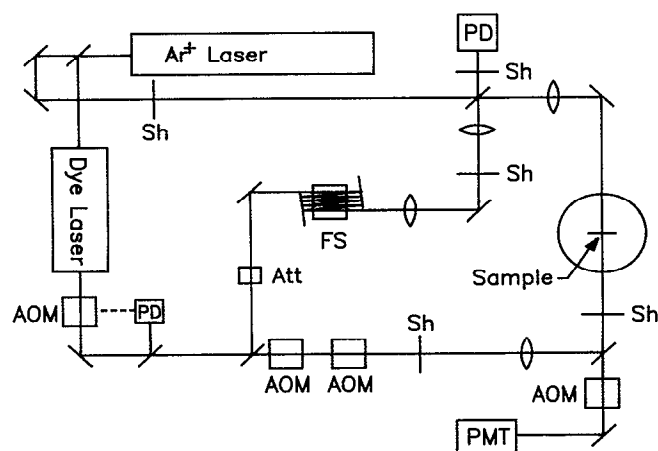


FIG. 1. Experimental apparatus used to record fast waiting-time-dependent optical holes. The dye laser output is split into burning and reading beams which run counterlinearly through the sample allowing continuous monitoring of the optical density (OD) after burning. The OD is monitored as a function of time at a number of discreet frequencies. Sh—shutter; AOM—acousto-optic modulator; Att—variable attenuator; FS—frequency shifter, a multipassed 300 MHz AOM; PD—photodiode; PMT—photomultiplier tube.

enough to diffract the beam up to five times in this fashion. Thus frequency shifts as large as  $\pm 1.5$  GHz could be obtained. Figure 2 is a plot of a permanent hole detected by scanning a 1.58 GHz shifted reading beam. The extra 80 MHz is due to the two 40 MHz AOM's in the burning beam. A permanent hole detected by scanning an unshifted beam would appear centered at zero offset. The apparent shift of the hole spectrum is 1.58 GHz.

Each pass through the frequency shifter distorted the beam profile somewhat so that by the fifth pass the beam profile was extremely non-Gaussian. Therefore, the beam was passed through a spatial filter before continuing. The spatial filter consisted of a 20 cm lens and a 100  $\mu\text{m}$  pinhole at the focus. All rings of the Airy pattern were blocked and only the central spot was allowed to pass. Not only did this clean up the beam profile, but it also had the advantage of making the focal characteristics of the beam independent of the frequency shift. This was critical to the acquisition of reliable data as will be discussed shortly.

Once the beams had passed through the modulating and shifting optics, as described above, they were focused onto the sample in a counterlinear fashion. The beam alignment was checked in two ways as is described below. Two different sets of spot sizes were used. In each, the burning-beam spot size was kept slightly larger than that of the reading beam to minimize the effect of pointing instabilities. The spot sizes used were 150 and 450  $\mu\text{m}$  for the burning beam and 135 and 365  $\mu\text{m}$  for the reading beam. Both sets of spot sizes gave identical results.

After the reading beam had passed through the sample, it was split off with a 50% beam splitter and sent into a cooled photomultiplier tube for detection. Because the burning beam was  $\sim 10^6$  times more intense than the reading beam, phototube pickup from scattered burning light could easily swamp the reading-beam signal. To protect the phototube from scattered light, the reading beam was passed

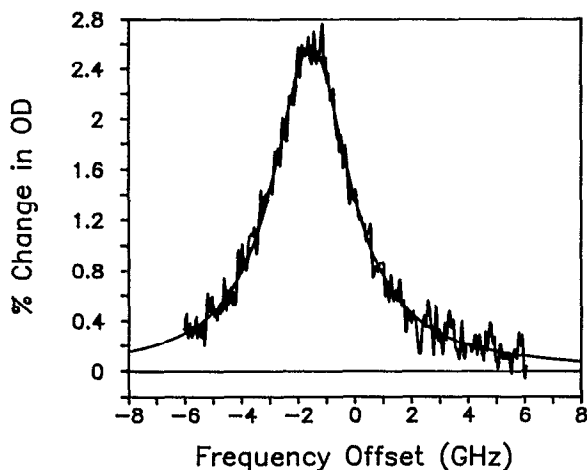


FIG. 2. Persistent hole spectrum showing the effectiveness of the frequency shifter. The hole was burned by irradiating the sample with the burning beam. The reading beam, which was shifted by the AOM 1.58 GHz relative to the burning beam, was then scanned. The hole shift is 1.58 GHz, indicating that there was negligible leakage from other laser frequencies and that the frequency shifting was accurate.

through an AOM which was turned off only during burning. The phototube signal, which was on the order of 5  $\mu\text{A}$ , was first put through a preamplifier (time response  $\sim 3 \mu\text{s}$ ). The amplified signal was then recorded by a 1 MHz, two-channel, 12-bit analog-to-digital converter (ADC), and stored. The second channel of the ADC was used to record the signal from a photodiode referenced to a pickoff directly before the cryostat. Following the acquisition of data, the computer divided the transmitted signal by the reference to correct for intensity fluctuations.

The burn-read sequence was as follows. Following a 100 ms read-beam exposure to determine the base-line transmission, a 10–100  $\mu\text{s}$  burn pulse generated a transient hole. No data could be recorded during burning due to the intense scattered light from the burning pulse. The phototube is protected from the scattered light by an AOM during burning. Immediately after burning, the read-beam transmission was monitored for up to 100 ms. The majority of the transient hole had decayed after 100 ms, and the hole had completely vanished after 1 s. After the transient hole had decayed, it left behind a small ( $\sim 0.03\%$ ) persistent hole. Therefore, holes could be burned repeatedly on the same spot without influencing the data. It was verified that the data were not dependent upon the number of repetitions when the number was less than 100.

After a small persistent hole had developed, the laser could be moved to a new position on the sample or to a new frequency. However, to increase the rate of acquisition, a hole-erasing procedure was used. Laser-induced hole filling has been reported by many authors, most notably Freary, Carter, and Small.<sup>52</sup> Irradiation of the sample at a wavelength other than that which burned the hole will, under certain conditions, reduce the hole area. To this end,  $\sim 250$  mW of argon-ion laser light was picked off before the dye laser and used as a periodic erasing beam. Figure 3 shows an example of the effect of hole erasing. A deep permanent hole is shown along with a scan through the same spectral range following erasing. With a spot diameter of  $\sim 2$  mm and an

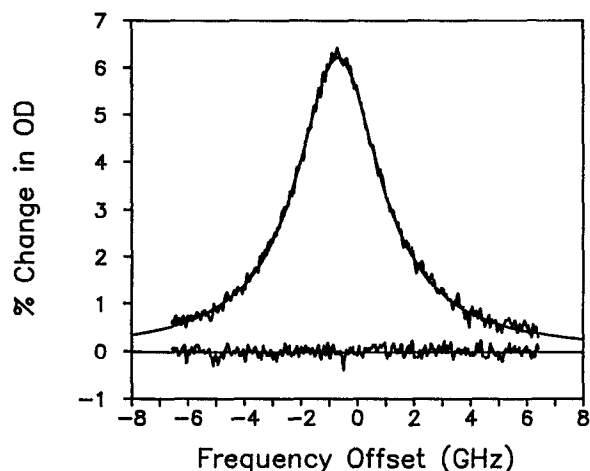


FIG. 3. Before and after scans showing effect of hole erasing. A deep permanent hole was burned. After a 10 s exposure of the 7 W/cm<sup>2</sup> argon ion laser, 100% of the hole is erased.

erasing time of  $\sim 10$  s, 100% of the hole was removed without influencing the results of the waiting-time-dependent experiments (as is shown below). Two shutters were added before the detectors to protect them from the  $\text{Ar}^+$  laser beam during erasing.

Before the data reported in the next section could be analyzed, it had to be determined whether the techniques reported here artificially influenced the results. The two significant differences between this method and that of standard hole burning are the burning conditions and the hole-erasing procedure. The burning and reading conditions are reported in Table I for the two sets of spot sizes used. Also reported is the maximum depth of the transient hole obtained for each power. Recall that both sets of spot sizes yielded identical results. Since the burning fluence, reading intensity, and burning intensity all differed by at least a factor of 2, effects such as local heating and saturation broadening were not a problem.

Nevertheless, a second test was performed as a check. Since repeated exposures of the burning beam created a persistent hole, the long-waiting-time hole width could be measured for holes burned with both cw and pulsed conditions. Figure 4(a) is a graph of a hole burned in the system cresyl violet in ethanol-*d* using a 100 s exposure of the read beam ( $15 \mu\text{W}/\text{cm}^2$ ). The approximate waiting time was 100 s. The hole width for this waiting time as reported in Ref. 1 is 2.96 GHz. The value reported in Fig. 4(a) is in accord with this. Figure 4(b) is a plot of a hole obtained with 100 pulses using the  $150 \mu\text{m}$  burning-beam spot size and the corresponding parameters as listed in Table I. The waiting time for this hole was also 100 s. The hole width is essentially unchanged and in excellent agreement with the low-power hole width reported earlier. Therefore, it may be concluded that the pulsed burning conditions used in this experiment did not artificially broaden the persistent holes. This supports the other tests which demonstrated the lack of artificial broadening of the transient holes.

The second question is whether erasing the persistent holes influenced the data. The transient absorption curves reported in the next section are the average of typically 1000 shots. After every 50–100 shots, the accumulated holes were erased with a 10 s exposure of the  $\text{Ar}^+$  laser beam followed by a 240 s pause when no data were collected. Figure 5(a) is a graph of a hole burned with a 100 s reading-beam exposure on a spot where several holes had been previously burned and erased. The waiting time was again 100 s. Note that the hole was burned 4 min after the last hole was erased. The

TABLE I. Burn times, burn fluences, and read powers used to create and detect spectral holes for cresyl violet in ethanol-*d* glass at 1.30 K.

Spot size <sup>a</sup> ( $\mu\text{m}$ )	Burn time ( $\mu\text{s}$ )	Fluence ( $\mu\text{J}/\text{cm}^2$ )	Transient <sup>b</sup> hole depth (%)	Reading-beam intensity ( $\mu\text{W}/\text{cm}^2$ )
150	10	50	1.5	15
450	100	100	2.2	1.4

<sup>a</sup> Diameter of the intensity.  
<sup>b</sup> Maximum depth achieved.

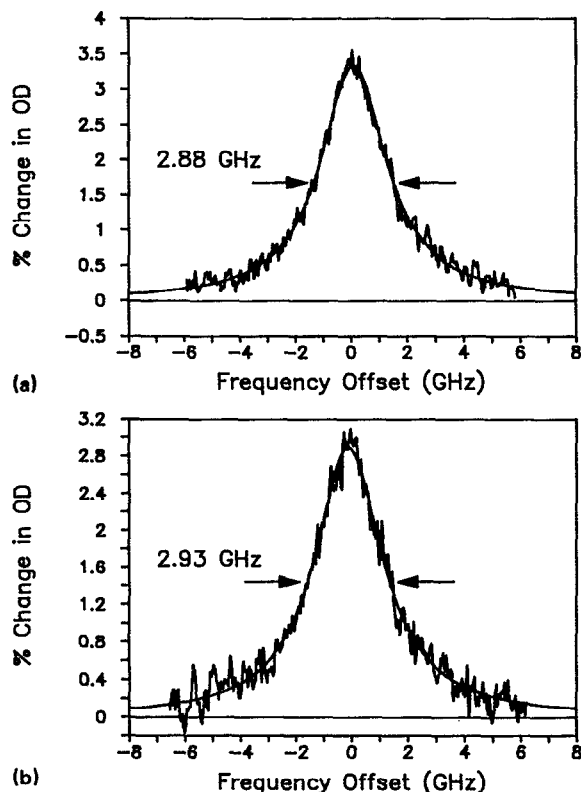


FIG. 4. Two persistent holes in cresyl violet in ethanol-*d* at 1.30 K showing that the measured hole widths are not dependent on the pulsed burning conditions used in this experiment. (a) Hole burned with a 100 s exposure of the weak cw reading beam. (b) Hole burned with 100 short, intense pulses of the burning beam. Both hole widths agree very well with the low-power hole width reported earlier for the same system and temperature.

hole width is again in very good agreement with the low-power, fresh spot hole width reported in Ref. 1 and above.

Figure 5(b) is a plot of a hole burned with 100 pulses of the  $150 \mu\text{m}$  burning beam on the same spot. The hole width is again in excellent agreement with the 100 s  $T_w$  hole width reported in Ref. 1 indicating that the hole-erasing process in no way influenced the data collected here. Figure 6 demonstrates the importance of waiting a finite amount of time after erasing before collecting data. The hole in Fig. 6, burned with pulsed conditions, also had a  $T_w = 100$  s but was burned only 20 s after erasing. The hole width is substantially broadened. The erasing beam was of sufficiently high power ( $\sim 7 \text{ W}/\text{cm}^2$ ) to modify, by heating or some other process, the internal glass structure slightly. Therefore, a sufficient amount of time had to pass before the internal structure of the glass relaxed back to the steady-state condition at 1.30 K.

Absorption vs waiting-time data were recorded for each of six different shifted burning frequencies. Note that the data were not recorded simultaneously, but that each shifted frequency was used one at a time. When changing from one frequency to another, the reading-beam direction shifted slightly. It was important to maintain good beam alignment. In a simple hole-burning experiment a single beam is used to burn and detect the holes. The alignment is never changed,

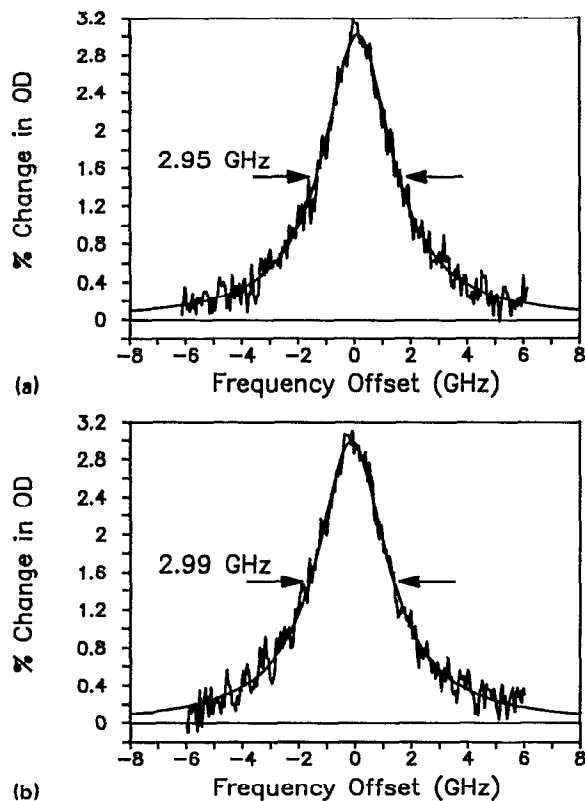


FIG. 5. Two persistent holes in cresyl violet in ethanol-*d* at 1.30 K showing that the measured hole widths are not dependent on the fact that the holes were periodically erased. (a) Hole burned with the weak cw beam on a spot where many holes had been previously burned and erased. (b) hole burned with 100 pulses of the burning beam on the same spot after the hole in (a) had been erased. The hole widths agree with the fresh spot (never burned) low-power hole widths reported earlier for the same system and temperature.

and the overlap between the burning and detection beams never varies. This is not true in a two-beam experiment such as this one. If the beam overlap from one frequency to another (or one day to another) is assumed to be constant but, in fact, varies, the data would be compromised. Changes in beam profile would cause similar problems. In these experiments both beam alignment and profile were kept as constant as possible. Small variations in overlap were present but were compensated for by periodically measuring the degree of overlap as is described below.

To assure that good overlap between reading and burning beams was maintained, 200  $\mu\text{m}$  (400  $\mu\text{m}$  for the larger spot size) pinholes on removable mounts were placed before and after the cryostat. By checking the transmission through the pinholes, the beams could be easily aligned. In addition, small changes in alignment were monitored in a straightforward way. Periodically during the acquisition of transient transmission data, a persistent hole was purposefully burned with a long exposure of the burning beam and was scanned with the reading beam. This was always done using a reproducible intensity and burn duration. The area of this persistent hole is directly proportional to the degree of overlap between the two beams at the sample. Thus, small drifts or misalignments could be effectively normalized out. As a

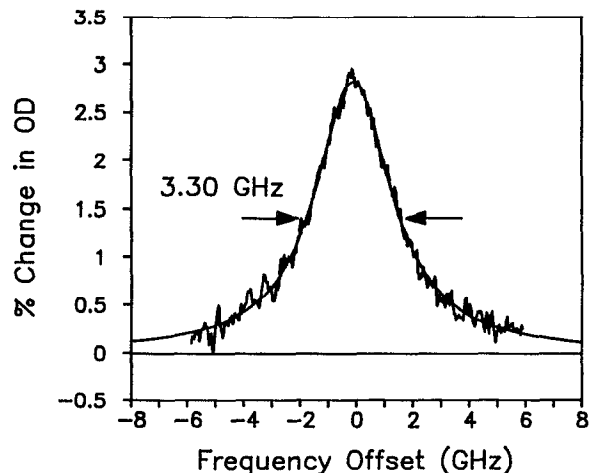


FIG. 6. A persistent hole in cresyl violet in ethanol-*d* at 1.30 K which was burned only 20 s after the previous hole was erased. The hole width is substantially broadened because the glass was not allowed to relax sufficiently after the erasing process. All other data reported here were recorded at least 240 s after any erasing. This interval was determined experimentally to be long enough to allow the system to totally relax following erasing to yield hole widths that are unperturbed by the erasing.

check of this procedure, after a transient transmission data set was collected, a second set was acquired with deliberately misaligned beams. By weighting the data sets linearly to the area of the "normalization" holes, the difference between the data sets was removed.

Once a complete set of transmission vs waiting-time data was acquired, it was converted to a set of 300 holes by taking time slices through the data. These holes were then fit by a least-squares method to generate the hole-width vs time data reported in the next section. Several data sets were collected to ensure reproducibility. Once reproducibility was confirmed, the data sets were averaged together.

### III. RESULTS AND DISCUSSION

Figure 7 shows change in optical density vs time curves for three of the six different read-beam shift frequencies—80 MHz, 680 MHz, and 1.28 GHz. The extra factor of 80 MHz is introduced by the two 40 MHz AOM's which modulate the burning beam. The solid lines through the data are best fits to a triple-exponential decay combined with a hole-broadening function. These fits were not used to calculate the hole-width vs time data presented below. The raw data were used instead.

Figure 8 is a plot of the hole area vs time calculated from the  $\Delta\text{OD}$  curves. The solid line is a fit to a triple exponential decay. The time scale studied in this measurement is in the range of the triplet lifetime of typical laser dyes. At low temperature, where spin-lattice relaxation is slow, three unequal triplet lifetimes are often observed.<sup>53</sup> The fact that the data may be fit to a triple exponential is consistent with, but does not prove, the notion that the transient holes observed here are caused by a triplet bottleneck with three different lifetimes. The best fit lifetimes are 60 ms, 1.5 ms, and 80  $\mu\text{s}$  with magnitudes roughly in the ratio 5:2:4.

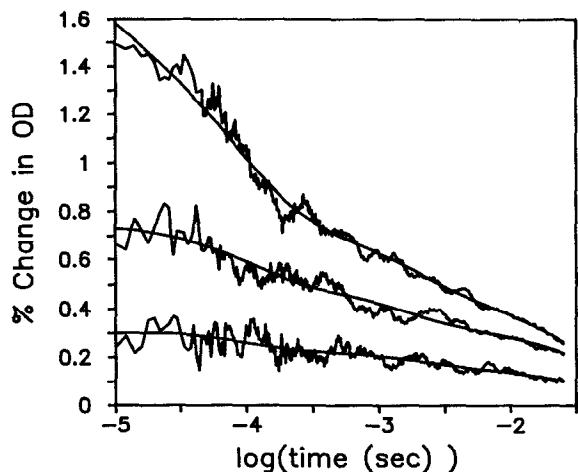


FIG. 7. Transient AOD plots for three different shifted reading-beam frequencies for the system cresyl violet in glassy ethanol-*d* at 1.30 K. Shift frequencies relative to burning beam: top, +80 MHz; middle, +680 MHz; and bottom, +1.28 GHz. The data are fit to a triple-exponential decay plus a hole broadening function to obtain information on the hole decay kinetics. The raw data was used to determine the hole widths as a function of time after burning.

It is possible that the transient hole is in some way related to the mechanism of persistent hole burning. The process of persistent hole burning is sometimes modeled as a hierarchical series of reactions.<sup>54</sup> The transient bleaching observed here could possibly be associated with photoinduced occupation of a preliminary state in the hole-burning pathway. It has been shown that for an ionic dye in ethanol the hole-burning mechanism involves double-proton transfers.<sup>55</sup> However, preliminary results indicate that the efficiency of transient bleaching, unlike that of persistent hole burning, is identical for both protonated and deuterated forms of ethanol glass. Unless the hypothesized preliminary step does not involve proton-deuteron exchange, it is more probable

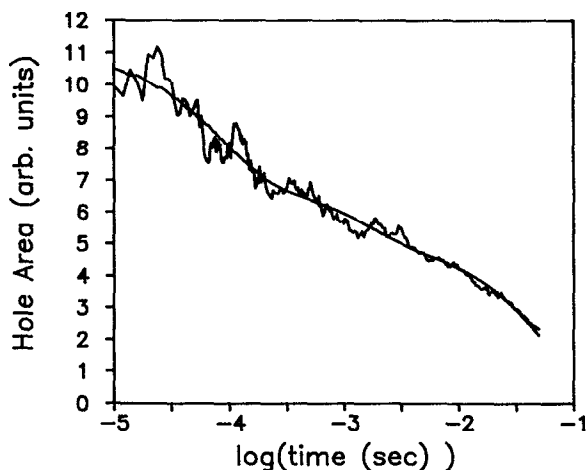


FIG. 8. Plot of the hole area vs log time for cresyl violet in ethanol-*d* at 1.30 K. The solid line is a fit to a triple-exponential decay (see text for values of the fit parameters). The fact that the data may be fit this way is consistent with the notion that the transient hole is due to a triplet bottleneck with three distinct triplet-spin sublevel lifetimes.

that the transient hole is indeed due to a triplet bottleneck.

Figure 9 shows two transient holes obtained at waiting times of 10 and 100  $\mu\text{s}$  for cresyl violet in ethanol-*d*. The solid lines are the best Lorentzian fits to the data. Figure 10 is a full plot of the hole-width vs log waiting time. As can be seen in the figure, the hole width shows a linear dependence on log time for waiting times between 10  $\mu\text{s}$  and 100 ms. The hole broadens by  $\approx 1$  GHz (almost a factor of 2) over this time span.

This logarithmic dependence on waiting time can be analyzed in terms of the theory of TLS-induced optical dephasing.<sup>1,38</sup> For  $T_w > 10\tau$  (the time between burning and reading the hole is much greater than a time on the order of the homogeneous dephasing time), the hole linewidth is given by

$$\Delta\omega_H \propto \int dR P(R) [1 - \exp(-RT_w)], \quad (1)$$

where  $R$  is the relaxation rate,  $T_w$  is the waiting time, and  $P(R)$  is the fluctuation rate distribution.<sup>37,38</sup> The constant of proportionality is a combination of temperature-independent constants such as the strength of the TLS-chromophore interaction. The dependence of  $\Delta\omega_H$  on  $T_w$  is found by differentiating Eq. (1) with respect to  $T_w$ . Performing this, one finds

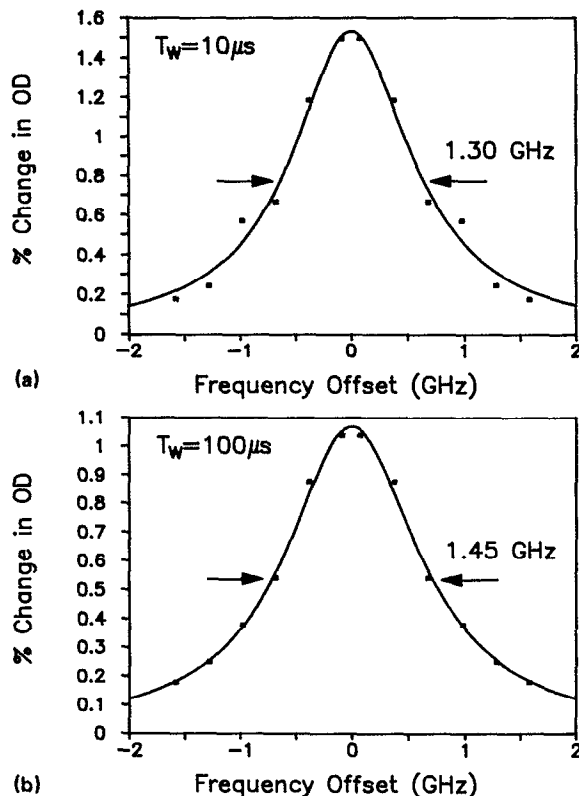


FIG. 9. Two holes burned in the system cresyl violet in ethanol-*d* glass at 1.30 K and recorded with different waiting times. The data were taken with positive frequency offsets and reflected through the line center to give the negative offset points. The solid lines are the best-fit Lorentzians to the data. The hole width can be seen to broaden with increased waiting time.

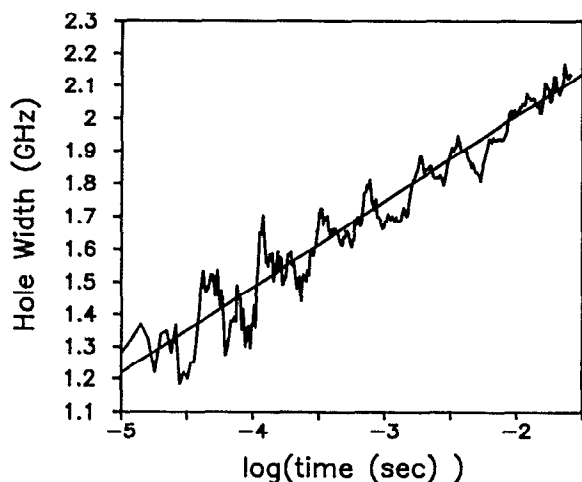


FIG. 10. Plot of hole width vs log time in seconds for cresyl violet in ethanol-*d* at 1.30 K. The fact that the data broaden linearly when plotted vs log time indicates that the fluctuation rate distribution is  $1/R$  in this region. The solid line is the best fit according to Eq. (1) using  $P(R) = 1/R$ . Over the time interval  $10\ \mu\text{s}$  to  $100\ \text{ms}$ , the hole broadens by almost a factor of 2. The broadening (spectral diffusion) is caused by the glass TLS dynamics occurring on the experimental time scale.

$$\frac{\partial(\Delta\omega_H)}{\partial T_w} \propto \int dR P(R) R \exp(-RT_w). \quad (2)$$

Thus the change in the linewidth with  $T_w$  is proportional to the LaPlace transform of  $R$  times the fluctuation rate distribution. If  $P(R)$  is proportional to  $1/R$ , it is straightforward to show that

$$\frac{\partial(\Delta\omega_H)}{\partial T_w} \propto 1/T_w, \quad (3)$$

or equivalently,

$$\frac{\partial(\Delta\omega_H)}{\partial \ln(T_w)} = \text{const.} \quad (4)$$

Thus, the fact that the hole linewidth broadens linearly with log time in Fig. 10 demonstrates that the fluctuation rate distribution,  $P(R)$ , is of the form  $1/R$  in this region.

Rationalization of a  $1/R$  distribution of fluctuation rates can be found in previous experimental as well as theoretical studies.<sup>30,44-48</sup> The original TLS model<sup>15,16</sup> hypothesized that there was a flat distribution of TLS tunneling parameters in glasses. The TLS relaxation rate is related to the tunneling parameters by

$$R \propto e^{-2\lambda}, \quad (5)$$

where  $\lambda$  is the tunneling parameter between the two wells of the TLS.<sup>56</sup> If  $P(\lambda) = \text{const.}$ ,

$$P(R) \propto \frac{\partial\lambda}{\partial R} \propto 1/R. \quad (6)$$

Thus a flat distribution of  $\lambda$  leads directly to a  $1/R$  distribution of  $P(R)$ . A microscopic physical explanation for a flat distribution of tunneling parameters does not currently exist. This is a problem of fundamental importance since this form of  $P(R)$ , with some modifications, has been used to describe many aspects of low-temperature glass dynam-

ics.<sup>15,16,44-47</sup> Inherent in a TLS model with a flat  $\lambda$  distribution is the existence of an upper and lower cutoff in the rate distribution, allowing for proper normalization of  $P(R)$ . With this in mind we will refer to  $P(R) \propto 1/R$  as a probability distribution. It was previously determined using two-pulse photon echoes that the fluctuation rate is  $1/R$  for large rates in many organic glasses including ethanol.<sup>30,33,48,57,58</sup> Previous hole-burning experiments in ethanol glass on longer time scales revealed a log normal distribution of rates. It is interesting to note that the log normal distribution, representative of a random event composed of a large series of independent subevents, asymptotically (large  $R$  limit) approaches  $1/R$ .<sup>59</sup> In fact, the larger the dispersion in the log normal distribution, the larger the range over which a  $1/R$  functionality is mimicked.

Combining the data of Ref. 1 for cresyl violet in ethanol at 1.30 K with the data taken here, it is possible to fit the entire  $T_w$  dependence from  $10\ \mu\text{s}$  to  $10\ 000\ \text{s}$  to a  $P(R)$  according to Eq. (1). This is plotted in Fig. 11. Over this time range the hole broadens by approximately a factor of 3. The solid line is a fit to the data according to Eq. (1) using a  $P(R)$  which goes as  $1/R$  for large rates and is log normal for slower rates. Explicitly, the data are fit to

$$\Delta\omega_H = \Delta\omega_0(R_{\text{max}}) + \int_{R_{\text{min}}}^{R_{\text{max}}} dR P(R) [1 - \exp(-RT_w)], \quad (7)$$

where  $P(R)$  is given by

$$P(R) = \frac{\Delta\omega_1}{R} H(R - R_1) + \frac{\Delta\omega_2}{\pi^{1/2} R \sigma} \times \exp\left[-\frac{(\ln R_0 - \ln R)^2}{\sigma^2}\right]. \quad (8)$$

$H$  is a step function such that  $H(x > 0) = 1, 0$  otherwise. The

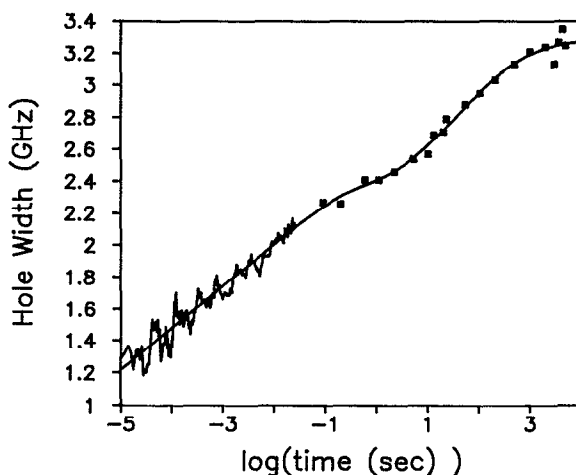


FIG. 11. Plot of hole width vs log time in seconds for cresyl violet in ethanol-*d* at 1.30 K. The data is plotted along with hole width results obtained earlier (■) for the same sample and temperature. Note that the new data fit smoothly into the data taken previously. The solid line is a fit according to Eqs. (7) and (8) (see text). Between  $10\ \mu\text{s}$  and  $10\ 000\ \text{s}$  the hole broadening (spectral diffusion) is almost a factor of 3.



integral in Eq. (7) is cut off at some  $R_{\max}$  such that  $R_{\max} \gg 1/T_w$  for all  $T_w$  studied in this experiment. This is done since (1) the behavior of  $\Delta\omega_H$  is not analytical for small  $T_w$ , and (2) the form of  $\Delta\omega_H$  is dependent only upon the area under the  $P(R)$  curve for  $R \gg 1/T_w$ . The results are independent of  $R_{\max}$  for a choice of  $R_{\max}$  that is sufficiently large. For the calculations reported here  $R_{\max}$  was set to  $e^{14} \text{ s}^{-1}$ . The parameters which give the best fit are  $\Delta\omega_0 = 860 \pm 20 \text{ MHz}$ ,  $\Delta\omega_1 = 115 \pm 2 \text{ MHz}$ ,  $\Delta\omega_2 = 970 \pm 50 \text{ MHz}$ ,  $\ln(R_0 \times 1 \text{ s}) = -4.1 \pm 0.7$ ,  $\ln(R_1 \times 1 \text{ s}) = 1.3 \pm 1.7$ , and  $\sigma = 3.3 \pm 0.9$ . The form of  $P(R)$  which best fits the data is plotted in Fig. 12. Thus  $P(R)$  has been determined for rates spanning nine decades.

The data reported in Figs. 11 and 12 almost suggest that the fluctuation rate distribution is  $1/R$  for all rates studied and not merely the faster rates. This is a valid point and is worth mentioning. If the only data considered were that of Fig. 11, a wholly  $1/R$  distribution would be a reasonable guess, and any deviations from that could be discounted as scatter. But, as the data collected on cresyl violet in ethanol and on resorufin in ethanol at 2.13 K show,<sup>1</sup> the S shape of the data in the long  $T_w$  region is not scatter—it is a real effect. Therefore, a distribution that is  $1/R$  for all rates should be discounted in favor of the distribution reported in Eq. (8) and Fig. 12.

Since the fluctuation rate distribution  $P(R)$  goes as  $1/R$  for  $10 \text{ s}^{-1} < R < 10^5 \text{ s}^{-1}$  and has also been determined to be  $1/R$  for rates in the region of the two-pulse photon echo,  $\sim 10^{10} \text{ s}^{-1}$ ,<sup>48</sup> it is reasonable to ask if  $P(R)$  mimicks  $1/R$  for all intermediate rates. If the fluctuation rate distribution determined for  $R < 10^5 \text{ s}^{-1}$  is extrapolated to the rate scale of the two-pulse echo, it should be possible to predict the value of the two-pulse echo and compare it to the experimental value. Note that the straight line in Figs. 10 and 11 cannot

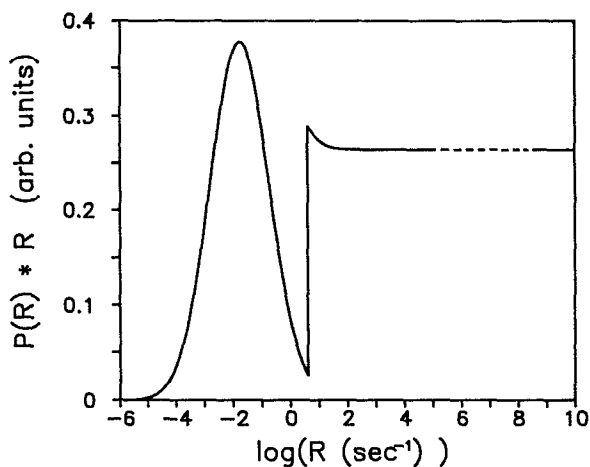


FIG. 12. Plot of  $P(R)*R$  vs  $\log R$  used to fit the data in Fig. 11.  $P(R)$  is  $1/R$  at large rates and cuts off to a log normal times  $1/R$  distribution at slow rates. See text for values of the parameters. The small rise at the slow end of the  $1/R$  distribution is from the tail of the log normal distribution. Extrapolating the  $1/R$  distribution to the time scale of the two-pulse echo gives good agreement with photon echo linewidth (see text). The part of the distribution obtained by extrapolation is shown as a dashed line.

simply be extrapolated back to the time scale of the echo for two reasons. First, the time scale of the two pulse echo is not a perfectly well-defined quantity.<sup>30,37,38</sup> Second, as was mentioned previously, the form of  $\Delta\omega_H$  for a  $1/R$  distribution and small  $T_w$  is not necessarily linear. To correctly calculate the echo linewidth, the four-point correlation function for a  $1/R$  distribution must be used.

It has been shown<sup>30,37</sup> that for a  $1/R$  distribution the four-point correlation functions that describe the tunneling TLS-induced hole-burning and photon echo linewidths are  $C(\tau, T_w, \tau) = \exp(-\beta\Theta\tau) \exp[-\beta\tau \ln(T_w/T_{PE})]$  (9) for  $T_w \gg T_{PE}$ , where  $T_{PE}$  is the two-pulse echo pure dephasing time, and

$$C(\tau, T_w, \tau) = \exp(-\beta\Theta\tau) \quad (10)$$

for  $T_w = 0$ , i.e., the two-pulse echo.  $\Theta$  is a constant equal to approximately 3.6.<sup>37</sup> The linewidths, or equivalently the decay of the polarizations, may be calculated from the correlation functions according to the simple relation<sup>30</sup>

$$P \propto \exp(-2\tau/T_2^*) \propto C(\tau, T_w, \tau), \quad (11)$$

where  $T_2^*$  is a pure dephasing time that depends on the time scale of the experiment. With use of Eqs. (9)–(11), it is possible to calculate the ratio of the linewidths for the echo and hole-burning experiments.<sup>30,37</sup> The result is

$$\Gamma_{\text{HB}}/\Gamma_{\text{PE}} = 1 + 1/\Theta \ln(T_w/T_{PE}). \quad (12)$$

Note that this result is equivalent to Eq. (4) in that it predicts a logarithmic time dependence of the hole width, but Eq. (12) is more general.

Comparing Eqs. (9) and (11), the value of  $T_{\text{HB}}$ , the pure dephasing time in a hole-burning experiment with waiting time  $T_w$ , for  $P(R) \propto 1/R$  is found to be

$$T_{\text{HB}} = \frac{2}{\beta [\Theta + \ln(T_w/T_{PE})]}. \quad (13)$$

Converting to a hole width according to the relation  $\Delta\omega_H = 2/(\pi T_{\text{HB}})$  and differentiating with respect to  $\ln(T_w)$  gives

$$\frac{\partial(\Delta\omega_H)}{\partial \ln(T_w)} = \beta/\pi. \quad (14)$$

Similarly, the dependence of the hole width for a distribution which is  $1/R$  may be calculated from Eq. (1). Setting the constant of proportionality to  $A$ , i.e.,

$$\Delta\omega_H = A \int dR 1/R [1 - \exp(-RT_w)], \quad (15)$$

one obtains the result

$$\frac{\partial(\Delta\omega_H)}{\partial \ln(T_w)} = A. \quad (16)$$

Comparing Eqs. (14) and (16), one obtains

$$A = \beta/\pi, \quad (17)$$

with use of Eqs. (10) and (11), the photon echo linewidth is found to be

$$\Gamma_{\text{PE}} = \frac{1}{\pi T_{\text{PE}}} = \frac{\beta\Theta}{2\pi}. \quad (18)$$

Combining Eqs. (17) and (18), one obtains the final result which relates the description of the hole linewidth given in Eq. (15) to the two-pulse echo linewidth,

$$\Gamma_{PE} = A\Theta/2. \quad (19)$$

Thus by fitting the data to the  $P(R)$  given in Eq. (8), it is possible to predict the linewidth of the two-pulse echo.  $\Delta\omega_1$  in Eq. (8) corresponds to  $A$  in Eq. (19). Therefore, the value of the echo linewidth predicted by the  $1/R$  distribution observed from 10  $\mu$ s to 100 ms is  $115 \times 3.6/2 = 207$  MHz. Adding in the lifetime contribution previously determined to be 28 MHz,<sup>48</sup> one obtains a linewidth of 235 MHz. The experimentally observed two-pulse echo linewidth for cresyl violet in deuterated ethanol at 1.30 K is 190 MHz.<sup>48</sup> The agreement is extremely good considering that there is scatter in both the hole-burning data and the echo data,<sup>48</sup> and the fact that the hole-burning data are being extrapolated over five decades in predicting the echo linewidth. Thus using millisecond time-scale hole-burning linewidths, it is possible to calculate subnanosecond time-scale photon echo decays.

The calculation of the photon echo results is dependent on the assumption that the  $1/R$  distribution continues unchanged past  $R = 100$  kHz to the region of the two-pulse echo. The close agreement between the calculated and experimental photon echo linewidths strongly supports the assumption that the fluctuation rate distribution is  $1/R$  in the range of rates  $10^{11} > R > 10^1$ . It is possible that the distribution is weighted toward smaller values of  $R$  as the lower than predicted echo linewidth suggests. This can be directly tested by performing  $T_w$ -dependent linewidth measurements for  $T_w$ s in the range  $10^{-9}$ – $10^{-5}$  s. In further support of a  $1/R$  rate distribution, linewidths obtained from two-pulse echo and stimulated echo measurements (weighting time of 25 ms) in zincporphin in ethanol and ethanol-*d* glasses resulted in a linewidth ratio of  $5.7 \pm 0.1$ .<sup>35</sup> This experimental result is in good agreement with that predicted by Eq. (12). Furthermore, these results (presented here and in Ref. 35) suggest the measured rate distribution to be independent of the chromophore.

#### IV. CONCLUDING REMARKS

These experimental results provide insight into the dynamics in low-temperature glasses. Many previous experiments on glasses have focused on a single quantity, i.e., a linewidth or a heat capacity, measured at a single waiting time. Such experiments reduce the entire range of dynamics to a single point. However, the key to understanding the dynamics of glasses and other complex systems lies in understanding the entire dynamical spectrum. The results reported in this paper have, for the first time, determined the fluctuation rate distribution over a very broad range of times, from picoseconds to thousands of seconds.

The fluctuation rate distribution is the dynamical spectrum of the material. Its form provides the distribution of tunneling parameters. Its temperature dependence can reveal the distribution of energy levels in the material. The results presented here yield the fluctuation rate distribution for ethanol glass at 1.3 K. The challenge now is to use the

type of  $T_w$ -dependent spectroscopy employed here to determine the dynamical spectrum of other glasses and other complex materials such as proteins. The broad  $1/R$  distribution measured for ethanol is reminiscent of the broad "1/f noise" spectra observed in electronic circuits. In general, inverse power law behavior like  $1/R$  (or  $1/R^{1+\alpha}$ ,  $0 < \alpha < 2$ ) must arise as limiting behavior of properly normalizable probability distributions (e.g., stable Levy distributions<sup>59</sup>) or be bounded between abrupt cutoffs. Photon echo experiments on a number of different glasses suggest that the  $1/R$  distribution is common, at least for the fast rates probed by photon echoes. If detailed  $T_w$ -dependent spectroscopic studies confirm the universal existence of broad  $1/R$  distributions for glasses and other disordered materials, a basic question will arise. What is the underlying universal property of disordered systems that gives them the same dynamical characteristics?

#### ACKNOWLEDGMENTS

This work was supported by the National Science Foundation Division of Materials Research (Grant No. DMR90-22675). Additional support was provided by the Office of Naval Research, Physics Division (Grant No. N000014-89-J1119). K. A. L. would like to thank AT&T Bell Laboratories for a Graduate Fellowship.

- <sup>1</sup> K. A. Littau, Y. S. Bai, and M. D. Fayer, *Chem. Phys. Lett.* **159**, 1 (1989); K. A. Littau, Y. S. Bai, and M. D. Fayer, *J. Chem. Phys.* **92**, 4145 (1990); K. A. Littau and M. D. Fayer, *Chem. Phys. Lett.* **176**, 551 (1991).
- <sup>2</sup> *Amorphous Solids: Low Temperature Properties*, edited by W. A. Phillips, (Springer, Berlin, 1981).
- <sup>3</sup> *Molecular Dynamics and Relaxation Phenomena in Glasses*, edited by T. Dorfmüller and G. Williams (Springer, Berlin, 1987); J. Wong and C. A. Angell, *Glass Structure by Spectroscopy* (Marcel Dekker, New York, 1976).
- <sup>4</sup> C. A. Angell, H. G. K. Sundar, A. R. Kulkarni, H. Senapati, and S. W. Martin, in *Molecular Dynamics and Relaxation Phenomena in Glasses*, edited by T. Dorfmüller and G. Williams (Springer, Berlin, 1987).
- <sup>5</sup> C. A. Angell, *Chem. Rev.* **90**, 523 (1990), and references therein.
- <sup>6</sup> S. M. Mahle and R. D. McCammon, *Phys. Chem. Glasses* **10**, 222 (1969).
- <sup>7</sup> M. von Schickfus and S. Hunklinger, *Phys. Lett.* **64A**, 144 (1977).
- <sup>8</sup> R. C. Zeller and R. O. Pohl, *Phys. Rev. B* **4**, 2029 (1971).
- <sup>9</sup> R. B. Stephens, *Phys. Rev. B* **8**, 289 (1973).
- <sup>10</sup> J. C. Lasjaunias, A. Ravex, and M. Vandorpe, *Solid State Commun.* **17**, 1045 (1975).
- <sup>11</sup> S. Kelham and H. M. Rosenberg, *J. Phys. C* **14**, 1737 (1981).
- <sup>12</sup> A. C. Anderson, W. Reese, and J. C. Wheatley, *Rev. Sci. Instrum.* **34**, 1386 (1963).
- <sup>13</sup> *Persistent Spectral Hole Burning: Science and Applications*, edited by W. E. Moerner (Springer, Berlin, 1988).
- <sup>14</sup> W. Breinl, J. Friedrich, and D. Haarer, *J. Chem. Phys.* **81**, 3915 (1984).
- <sup>15</sup> P. W. Anderson, B. I. Halperin, and C. M. Varma, *Philos. Mag.* **25**, 1 (1972).
- <sup>16</sup> W. A. Phillips, *J. Low Temp. Phys.* **7**, 351 (1972).
- <sup>17</sup> W. M. Goubau and R. H. Tait, *Phys. Rev. Lett.* **34**, 1220 (1975).
- <sup>18</sup> J. L. Black and B. I. Halperin, *Phys. Rev. B* **16**, 2879 (1984).
- <sup>19</sup> J. E. Lewis, J. C. Lasjaunias, and G. Shumacher, *J. Phys. (Paris)* **39**, Suppl. C6-967 (1978).
- <sup>20</sup> M. T. Lopenon, R. C. Dynes, V. Narayanamurti, and J. P. Garno, *Phys. Rev. Lett.* **45**, 457 (1980).
- <sup>21</sup> R. B. Kummer, R. C. Dynes, and V. Narayanamurti, *Phys. Rev. Lett.* **40**, 1187 (1978).
- <sup>22</sup> B. Golding and J. E. Graebner, *Phys. Rev. Lett.* **37**, 852 (1976).
- <sup>23</sup> B. Golding, J. E. Graebner, B. I. Halperin, and R. J. Schultz, *Phys. Rev. Lett.* **30**, 223 (1973).

- <sup>24</sup> W. Arnold, S. Hunklinger, S. Stein, and K. Dransfeld, *J. Non-Cryst. Solids* **14**, 192 (1974).
- <sup>25</sup> J. Jäckle, L. Piché, W. Arnold, and S. Hunklinger, *J. Non-Cryst. Solids* **20**, 365 (1978).
- <sup>26</sup> J. M. Hayes, R. Jankowiak, and G. J. Small, in *Persistent Spectral Hole Burning: Science and Applications*, edited by W. E. Moerner (Springer, Berlin, 1988).
- <sup>27</sup> R. Jankowiak and G. J. Small, *Science* **237**, 618 (1987).
- <sup>28</sup> J. Jäckle and K. L. Jüngst, *Z. Phys. B* **30**, 243 (1978).
- <sup>29</sup> T. B. Tamm and P. M. Saari, *Opt. Spectrosc.* **40**, 395 (1976); P. M. Saari and T. B. Tamm, *ibid.* **38**, 594 (1975); *Chem. Phys. Lett.* **30**, 219 (1975).
- <sup>30</sup> M. Berg, C. A. Walsh, L. R. Narasimhan, K. A. Littau, and M. D. Fayer, *J. Chem. Phys.* **88**, 1564 (1988).
- <sup>31</sup> H. Fidder, S. DeBoer, and D. A. Wiersma *Chem. Phys.* **139**, 317 (1989).
- <sup>32</sup> A. Rebane and D. Haarer, *Opt. Commun.* **70**, 478 (1989).
- <sup>33</sup> C. A. Walsh, M. Berg, L. R. Narasimhan, and M. D. Fayer, *J. Chem. Phys.* **86**, 77 (1987); M. Berg, C. A. Walsh, L. R. Narasimhan, K. A. Littau, and M. D. Fayer, *Chem. Phys. Lett.* **139**, 66 (1987).
- <sup>34</sup> M. M. Broer, B. Golding, W. H. Haemmerle, J. R. Simpson, and D. L. Huber, *Phys. Rev. B* **33**, 4160 (1986).
- <sup>35</sup> Hans C. Meijers and Douwe A. Wiersma, *Chem. Phys. Lett.* **181**, 318 (1991).
- <sup>36</sup> L. R. Narasimhan, Y. S. Bai, M. A. Dugan, and M. D. Fayer, *Chem. Phys. Lett.* **176**, 335 (1991).
- <sup>37</sup> Y. S. Bai and M. D. Fayer, *Chem. Phys.* **128**, 135 (1988); *Comments Condensed Matter Phys.* **14**, 343 (1989).
- <sup>38</sup> Y. S. Bai and M. D. Fayer, *Phys. Rev. B* **39**, 11 066 (1989).
- <sup>39</sup> S. Jahn, D. Haarer, and B. M. Karlamov, *Chem. Phys. Lett.* **181**, 31 (1991).
- <sup>40</sup> H. Scher, M. F. Shlesinger, and J. T. Bendler, *Phys. Today* **44** (No. 1), 26 (1991), and references therein.
- <sup>41</sup> H. P. H. Thijssen, A. I. M. Dicker, and S. Völker, *Chem. Phys. Lett.* **92**, 7 (1982).
- <sup>42</sup> H. P. H. Thijssen, R. van den Berg, and S. Völker, *Chem. Phys. Lett.* **97**, 295 (1983).
- <sup>43</sup> R. van den Berg, A. Visser, and S. Völker, *Chem. Phys. Lett.* **144**, 105 (1988).
- <sup>44</sup> D. L. Huber, M. M. Broer, and B. Golding, *Phys. Rev. Lett.* **52**, 2281 (1984); W. O. Putikka and D. L. Huber, *Phys. Rev. B* **36**, 3436 (1987).
- <sup>45</sup> R. Jankowiak, G. J. Small, and K. B. Athreya, *J. Phys. Chem.* **90**, 3896 (1986).
- <sup>46</sup> R. Jankowiak and G. J. Small, *J. Phys. Chem.* **90**, 5612 (1986).
- <sup>47</sup> S. K. Lyo and R. Orbach, *Phys. Rev. B* **22**, 4223 (1980).
- <sup>48</sup> L. R. Narasimhan, D. W. Pack, and M. D. Fayer, *Chem. Phys. Lett.* **152**, 287 (1988); D. W. Pack, L. R. Narasimhan, and M. D. Fayer, *J. Chem. Phys.* **92**, 4125 (1990).
- <sup>49</sup> O. Haida, H. Suga, and S. Seki, *J. Chem. Thermochem.* **9**, 1113 (1977).
- <sup>50</sup> R. van den Berg and S. Völker, *Chem. Phys. Lett.* **137**, 201 (1987).
- <sup>51</sup> M. Lindrum, and B. Nickel, *Chem. Phys.* **144**, 129 (1990), and references therein.
- <sup>52</sup> B. L. Fearey, T. P. Carter, and G. J. Small, *Chem. Phys.* **101**, 279 (1986).
- <sup>53</sup> R. Avarmaa, *Chem. Phys. Lett.* **46**, 279 (1977).
- <sup>54</sup> L. Shu and G. J. Small, *Chem. Phys.* **141**, 447 (1990).
- <sup>55</sup> F. Kokai, H. Tanaka, J. I. Brauman, and M. D. Fayer, *Chem. Phys. Lett.* **143**, 1 (1988).
- <sup>56</sup> B. Golding and J. E. Graebner, in *Amorphous Solids: Low Temperature Properties*, edited by W. A. Phillips (Springer, Berlin, 1981).
- <sup>57</sup> S. R. Greenfield, Y. S. Bai, and M. D. Fayer, *Chem. Phys. Lett.* **170**, 133 (1990).
- <sup>58</sup> A. Elschner, L. R. Narasimhan, and M. D. Fayer, *Chem. Phys. Lett.* **171**, 19 (1990).
- <sup>59</sup> E. W. Montroll and M. F. Shlesinger, *J. Stat. Phys.* **32**, 209 (1983); B. H. Hughes, M. F. Shlesinger, and E. W. Montroll, *Proc. Natl. Acad. Sci. USA* **75**, 3287 (1981); E. W. Montroll and M. F. Shlesinger, *ibid.* **79**, 3380 (1982).